

Comparison of Damping Models for Space Flight Cables

Kaitlin Spak, PhD Candidate, Virginia Tech, Blacksburg, VA
kspak@vt.edu

Gregory Agnes, R&D Engineer, Jet Propulsion Laboratory, California Institute of Technology,
Pasadena, CA

Daniel Inman, Department of Aerospace Engineering, University of Michigan, Ann Arbor, MI

NOMENCLATURE

$\alpha, \beta, a_i, b_i, \gamma, \delta$	Dissipation function / history kernel constants
A	Cross-sectional area
A_b, B_b, D_d	Dimensionless damping parameters defined within
C	Dimensionless hysteretic damping parameter containing dissipation function
c_a	Shear damping coefficient
c_b	Rotational damping coefficient
E	Elastic modulus
F	Transfer function matrix for use in distributed transfer function method
G	Shear modulus
$G(s)$	Dissipation function (transformed into Laplace domain)
I	Moment area of inertia
K	Shear coefficient
L	Beam length
M, N	Left and right boundary condition matrices for distributed transfer function method
P_1, P_2	Dimensionless beam parameters for bending and rotation, respectively, defined within
T	Axial tension in cable
T_s	Dimensionless tension parameter
t	Time coordinate
s	Laplace transformed time coordinate
w	Beam displacement as a function of time and distance
x	Spatial coordinate; distance along the beam in the axial direction
η	State space vector of displacement solution and derivatives for distributed transfer function method
ρ	Density
ψ	Total beam rotation
$\tau = \sqrt{\frac{\rho AL^4}{EI}}$	Time parameter

ABSTRACT

A model to predict the dynamic response of space flight cables is developed. Despite the influence of cable harnesses on space structures' dynamics, a predictive model for quantifying the damping effects is not available. To further this research, hysteretic and proportional viscous damping were incorporated in Euler-Bernoulli and Timoshenko beam models to predict the dynamic response of a typical space flight cable, using hysteretic dissipation functions to characterize the damping mechanism. The Euler-Bernoulli beam model was used to investigate the hysteresis functions specifically, and it was determined that including hysteretic dissipation functions in the equations of motion was not sufficient to model the

additional modes arising in damped cables; additional damping coordinates in the method of Golla, Hughes and McTavish will be necessary to predict damping behavior when using dissipation functions for this case. A Timoshenko model that included viscous and time hysteresis damping was developed as well, and will ultimately be more appropriate for cable modeling due to the inclusion of shear and rotary inertia terms and damping coefficients.

Keywords: Cable modeling, cable damping, time hysteresis, dissipation functions, cable vibration

INTRODUCTION

Modern space structures are lighter and more complex than heritage systems. Power and signal cables are vital components that may not be incorporated into modal testing until the spacecraft is nearly ready for launch. At that development stage, finding out that the addition of cables will cause unwanted resonance is problematic and costly to fix. Alternatively, knowing that cables can add quantifiable and predictable damping to the structure can reduce costs by reducing the need for additional damping treatments.

The cables used on spacecraft vary in terms of size, construction, and insulation. Much research has been done on modeling the dynamic response of cables, with less research available on cable damping, and still less regarding damping of structures due to the addition of cable harnesses. In order to reach the goal of predicting the damping effects of structures due to cables, determining the damping quality inherent in the cable itself is a first step.

In this paper, a method to model the dynamic response of a space-flight cable, including damping effects, is developed. Comparison to experimental data to establish its validity and usefulness as a predictor for cable damping ratios is reserved for future work.

BACKGROUND

Past research on cable damping generally aims to model either the frictional forces between each instance of contact between wires, or tries to quantify the changes in bending stiffness as the cable changes curvature. The earliest cable models were known as fiber models; these models were similar to string models and assumed no bending stiffness of the cable. It did not take long to determine that bending stiffness was important in cable motion, especially for larger and thicker cables, and thin rod models were developed. The thin rod formulation models each individual cable as a helical rod wrapped around a straight core [1]. Thin rod models determined stress and strain well, but to determine vibration response, beam models that included bending stiffness gave more direct results. Later, semi-continuous models, in which each layer of wires was homogenized into a cylinder, were developed [2].

Since the global behavior of the cable is most of interest for this particular application, this model will not rely on the individual forces between the wires. Instead, the cable will be modeled as a homogenous beam with properties to be determined experimentally. This paper investigates the inclusion of shear, rotary inertia, and axial tension terms, all of which are generally ignored in previous cable models. The other focus of this paper is incorporating a time hysteresis damping term employed to model the internal damping inherent in the cable.

Hysteretic damping was investigated based on the observation that viscous damping alone is not sufficient to model the damping of a slack cable. Spacecraft cables are usually attached with excess slack (no tension) to prevent connectors from becoming loose or disconnected due to strain from the cable tension. In prior experiments, cable frequencies decreased predictably as tension decreased until the cable became slack, at which point the cable response became significantly different as shown by the solid line in Figure 1. To predict the effects of cable harnesses attached to space structures, a model to characterize slack cables must be developed. The bending stiffness inherent in cable harnesses for spacecraft makes slack string models inappropriate for cable harnesses in these cases. The axial tension term is included in the equations of motion in an effort to investigate if attaching cables to spacecraft with a very low tension could lead to more accurate response predictions. Figure 2 shows a rough comparison between the experimental cable data from previous experiments for a slack cable and the undamped and viscously damped cable models [3]. It is important to note that only a cursory attempt was made to match model properties to the cable properties exactly. Copper properties were used to approximate the cable wire

properties, and boundary conditions were matched. Jacketing of the wire was not taken into account for the model. It is clear that including only viscous damping will not show the frequency shifts and changes that the slack cable exhibits due to damping.

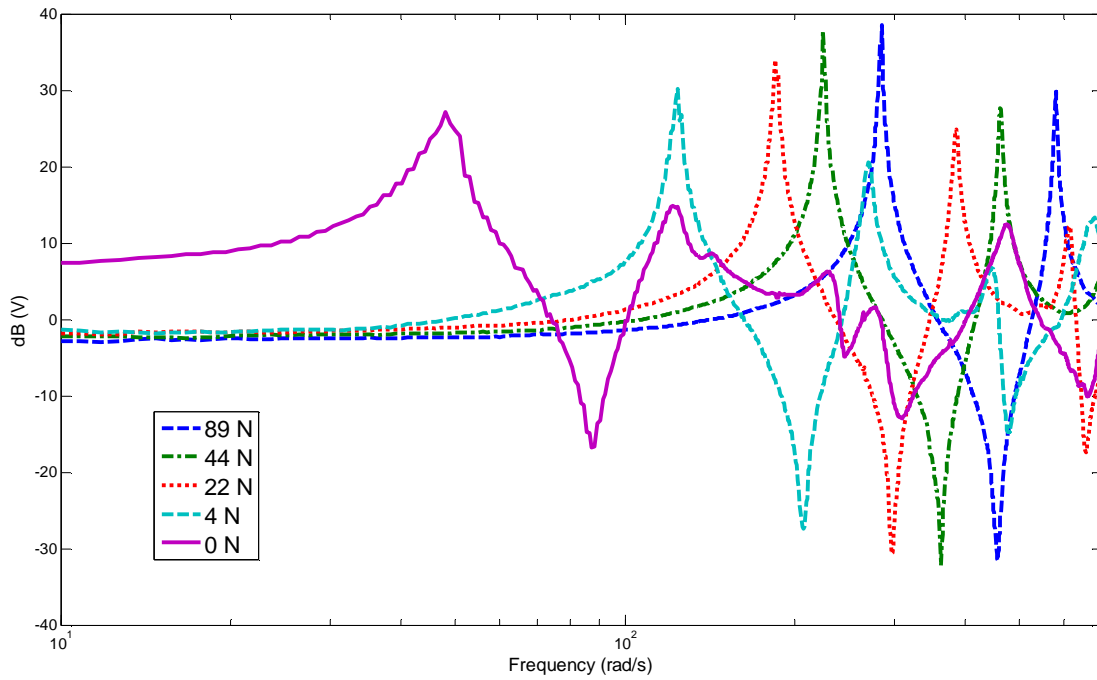


Fig. 1 Experimentally determined frequency response of a cable for various tensions; the frequencies shift and change and damping increases appreciably for the slack cable [3]

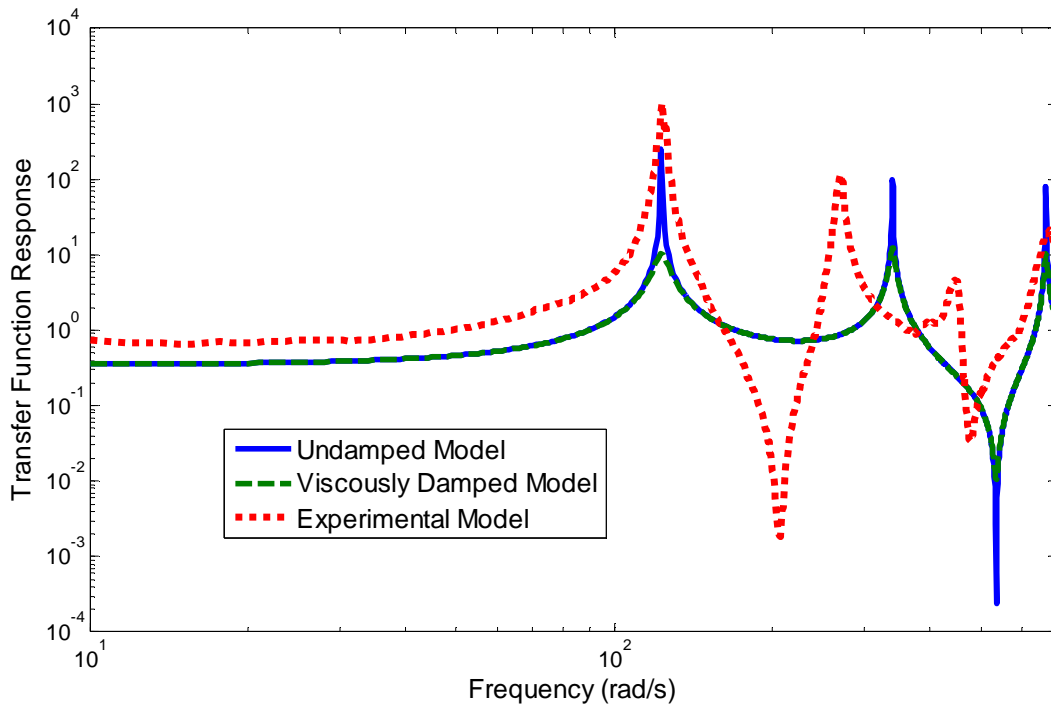


Fig. 2 Rough comparison of experimental response of cable under 4 N tension to undamped cable model and viscously damped cable model, showing the inadequacy of the viscously damped Euler-Bernoulli cable model for this application

EQUATIONS OF MOTION

To incorporate time hysteresis, a simple Euler-Bernoulli beam model was studied initially. Although research shows that cables are best modeled by including shear effects, these are neglected in the Euler-Bernoulli model as a first step to investigate the effects of the hysteretic damping only. The distributed transfer function method (DTFM) used for solutions is computationally intensive when the transfer function matrix includes more terms, so limiting the number of terms by using the Euler-Bernoulli model provides a reasonable starting point. Once results were achieved with the Euler-Bernoulli model, shear and rotational inertia terms were added to incrementally increase the complexity of the problem and yield a baseline viscous damping Timoshenko model and the ultimately desired hysteretically damped Timoshenko model.

Euler-Bernoulli Time Hysteresis Model

This simple beam model includes viscous damping, axial tension, and a time hysteresis term (which is composed of a time-dependent dissipation function or history kernel $g(t)$ discussed later, and spatial derivatives). This is also known as Boltzmann-type viscoelasticity [4].

$$\rho A \frac{\partial^2 w}{\partial t^2} + c_a \frac{\partial w}{\partial t} + EI \frac{\partial^4 w}{\partial x^4} - T \frac{\partial^2 w}{\partial x^2} - \frac{\partial^2}{\partial x^2} \int_0^t g(t) \frac{\partial^2 w}{\partial x^2} dt = 0$$

Here, $w = w(x, t)$ is the transverse displacement of the cable and is a function of time, t , and distance, x . This equation is non-dimensionalized, rearranged, and transformed into the Laplace domain to facilitate the transfer function formulation:

$$\begin{aligned} \rho A \frac{L}{\tau^2} \frac{\partial^2 w}{\partial t^2} + c_a \frac{L}{\tau} \frac{\partial w}{\partial t} + EI \frac{L}{L^4} \frac{\partial^4 w}{\partial x^4} - T \frac{L}{L^2} \frac{\partial^2 w}{\partial x^2} - \frac{1}{L^2} \frac{\partial^2}{\partial x^2} \int_0^t g(t) \frac{L}{L^2} \frac{\partial^2 w}{\partial x^2} \tau dt = 0 \\ \frac{\partial^4 W}{\partial x^4} - \frac{\tau}{EI} \frac{G(s)}{s} \frac{\partial^4 W}{\partial x^4} = - \frac{\rho A L^4}{EI \tau^2} s^2 W - c_a \frac{L^4}{EI \tau} s W + \frac{TL^2}{EI} \frac{\partial^2 W}{\partial x^2} \\ \frac{\partial^4 W}{\partial x^4} = \left(\frac{1}{1 - \frac{C}{s}} \right) \left(-s^2 W - D_d s W + T_s \frac{\partial^2 W}{\partial x^2} \right) \end{aligned}$$

Where the dimensionless parameters used are defined as:

$$D_d = \frac{c_a L^4}{EI \tau}, \quad T_s = \frac{TL^2}{EI}, \text{ and } C = G(s) \frac{\tau}{EI}$$

This simple model could be run quickly to show differences due to different damping formulations, but as mentioned, cables are more accurately modeled as shear beams rather than Euler-Bernoulli beams [5]. The beam equation used from this point forward includes both rotary and shear terms (Timoshenko formulation), since the cables are flexible enough to rotate appreciably and must incorporate shear effects. In addition, since preliminary experiments showed vibration response to vary with cable tension, this aspect has also been included, though not varied for the simulations presented here.

Timoshenko Viscous Model

The simplest and most commonly used damping model is a viscous-proportional damping model in which changes in the displacement or rotation over time are multiplied by a damping coefficient. Internal material damping within the wires and damping due to contact effects between the wires are both expected damping mechanisms. In this case, damping for the displacement and rotation is included, and gives these starting equations:

$$\begin{aligned} \rho A \frac{\partial^2 w}{\partial t^2} + c_a \frac{\partial w}{\partial t} &= \kappa AG \frac{\partial^2 w}{\partial x^2} - \kappa AG \frac{\partial \psi}{\partial x} \\ \rho I \frac{\partial^2 \psi}{\partial t^2} + c_b \frac{\partial \psi}{\partial t} + T \frac{\partial w}{\partial x} &= EI \frac{\partial^2 \psi}{\partial x^2} + \kappa AG \frac{\partial w}{\partial x} - \kappa AG \psi \end{aligned}$$

Which are combined, non-dimensionalized and rearranged to facilitate the transfer function formulation, yielding:

$$\frac{\partial^4 w}{\partial x^4} = \frac{\rho L^2}{E \tau^2} \frac{\partial^4 w}{\partial x^2 \partial t^2} + \frac{\rho L^2}{K G \tau^2} \frac{\partial^4 w}{\partial x^2 \partial t^2} + \frac{c_a L^2}{K A G \tau} \frac{\partial^3 w}{\partial x^2 \partial t} + \frac{c_b L^2}{E I \tau} \frac{\partial^3 w}{\partial x^2 \partial t} + \frac{T L^2}{E I} \frac{\partial^2 w}{\partial x^2} - \frac{\rho^2 L^4}{K G E \tau^4} \frac{\partial^4 w}{\partial t^4} - \frac{c_a \rho L^4}{K A G E \tau^3} \frac{\partial^3 w}{\partial t^3} - \frac{c_b \rho L^4}{K G E I \tau^3} \frac{\partial^3 w}{\partial t^3} - \frac{c_a c_b L^4}{K A G E I \tau^2} \frac{\partial^2 w}{\partial t^2} - \frac{\rho A L^4}{E I \tau^2} \frac{\partial^2 w}{\partial t^2} - \frac{c_a L^4}{E I \tau} \frac{\partial w}{\partial t}$$

Non-dimensional parameters are chosen and the Laplace transform is performed:

$$\frac{\partial^4 W}{\partial x^4} = (P_1 s^2 + P_2 s^2 + A_d s + B_d s + T_s) \frac{\partial^2 W}{\partial x^2} + (-P_1 P_2 s^4 - A_d P_1 s^3 - B_d P_2 s^3 - A_d B_d s^2 - s^2 - D_d s) W$$

Where the dimensionless parameters used here are defined as:

$$A_d = \frac{c_a L^2}{K A G \tau}, \quad B_d = \frac{c_b L^2}{E I \tau}, \quad P_1 = \frac{\rho L^2}{E \tau^2}, \quad P_2 = \frac{\rho L^2}{K G \tau^2}, \quad D_d = \frac{c_a L^4}{E I \tau}, \quad T_s = \frac{T L^2}{E I}, \text{ and } C = G(s) \frac{\tau}{E I}$$

This model is included to provide a baseline damping value. The following models presented are more complex to analyze, but may provide greater agreement with physical reality.

Timoshenko Time Hysteresis Models

A time hysteresis model includes a damping term that takes the past strain history of the structure into account. The authors were interested in whether internal damping occurred because of internal shear or internal rotation, so two models were developed; one with the time hysteresis due to the rotation only $\left(\frac{\partial w}{\partial x}\right)$, and one with the time hysteresis due to the shear angle (ψ) . The $g(t)$ term is a time-dependent expression that can take a variety of forms with the physical assumption being that the stress in the cable is proportional not only to the strain, but the past strain as well. Time hysteresis damping has traditionally been used with the Boltzmann damping formulation [6], but the dissipation function used by Golla and Hughes was also investigated with these models [7]. Since the time hysteresis damping should be describing only the internal damping, the viscous damping terms are included as well to account for the damping due to the motion of the cable in the air.

The first hysteretic model incorporates time hysteresis acting on $\frac{\partial^2 w}{\partial x^2}$, the strain of the cable due to bending. The time hysteresis term is added to the second equation as shown and the integral is taken care of through the Laplace transformation necessary for the distributed transfer function method used to determine the solution and described in the next section. The end result is a Laplace transform of the equation of motion with the non-dimensional parameters included as the coefficients:

$$\begin{aligned} \rho A \frac{\partial^2 w}{\partial t^2} + c_a \frac{\partial w}{\partial t} &= \kappa A G \frac{\partial^2 w}{\partial x^2} - \kappa A G \frac{\partial \psi}{\partial x} + q(x, t) \\ \rho I \frac{\partial^2 \psi}{\partial t^2} + c_b \frac{\partial \psi}{\partial t} + T \frac{\partial w}{\partial x} &= E I \frac{\partial^2 \psi}{\partial x^2} + \kappa A G \frac{\partial w}{\partial x} - \kappa A G \psi - \frac{\partial}{\partial x} \int_0^t g(t - \tau) \frac{\partial^2 w}{\partial x^2} dt \end{aligned}$$

$$\frac{\partial^4 w}{\partial x^4} = \frac{\rho L^2}{E \tau^2} \frac{\partial^4 w}{\partial x^2 \partial t^2} + \frac{\rho L^2}{K G \tau^2} \frac{\partial^4 w}{\partial x^2 \partial t^2} + \frac{c_a L^2}{K A G \tau} \frac{\partial^3 w}{\partial x^2 \partial t} + \frac{c_b L^2}{E I \tau} \frac{\partial^3 w}{\partial x^2 \partial t} + \frac{T L^2}{E I} \frac{\partial^2 w}{\partial x^2} - \frac{\rho^2 L^4}{K G E \tau^4} \frac{\partial^4 w}{\partial t^4} - \frac{c_a \rho L^4}{K A G E \tau^3} \frac{\partial^3 w}{\partial t^3} - \frac{c_b \rho L^4}{K G E I \tau^3} \frac{\partial^3 w}{\partial t^3} - \frac{c_a c_b L^4}{K A G E I \tau^2} \frac{\partial^2 w}{\partial t^2} - \frac{\rho A L^4}{E I \tau^2} \frac{\partial^2 w}{\partial t^2} - \frac{c_a L^4}{E I \tau} \frac{\partial w}{\partial t} + \frac{\tau}{E I} \frac{\partial^2}{\partial x^2} \int_0^t g(t - \tau) \frac{\partial^2 w}{\partial x^2} dt$$

$$\frac{\partial^4 W}{\partial x^4} = \frac{(P_1 s^2 + P_2 s^2 + A_d s + B_d s + T_s) \partial^2 W}{1 - \frac{C}{s}} + \frac{(-P_1 P_2 s^4 - A_d P_1 s^3 - B_d P_2 s^3 - A_d B_d s^2 - s^2 - D_d s) W}{1 - \frac{C}{s}}$$

The next hysteretic model includes time hysteresis acting on psi, the total rotation of the beam. The same steps are followed and the same non-dimensional parameters substituted to yield the Laplace transform of the damped equation of motion.

$$\begin{aligned} \rho A \frac{\partial^2 w}{\partial t^2} + c_a \frac{\partial w}{\partial t} &= \kappa A G \frac{\partial^2 w}{\partial x^2} - \kappa A G \frac{\partial \psi}{\partial x} + q(x, t) \\ \rho I \frac{\partial^2 \psi}{\partial t^2} + c_b \frac{\partial \psi}{\partial t} + T \frac{\partial w}{\partial x} &= EI \frac{\partial^2 \psi}{\partial x^2} + \kappa A G \frac{\partial w}{\partial x} - \kappa A G \psi - \frac{\partial}{\partial x} \int_0^t g(t-\tau) \frac{\partial \psi}{\partial x} dt \end{aligned}$$

Equations are combined and rearranged:

$$\begin{aligned} \frac{\partial^4 w}{\partial x^4} &= \frac{\rho L^2}{E \tau^2} \frac{\partial^4 w}{\partial x^2 \partial t^2} + \frac{\rho L^2}{K G \tau^2} \frac{\partial^4 w}{\partial x^2 \partial t^2} + \frac{c_a L^2}{K A G \tau} \frac{\partial^3 w}{\partial x^2 \partial t} + \frac{c_b L^2}{EI \tau} \frac{\partial^3 w}{\partial x^2 \partial t} + \frac{T L^2}{EI} \frac{\partial^2 w}{\partial x^2} - \frac{\rho^2 L^4}{E K G \tau^4} \frac{\partial^4 w}{\partial t^4} - \frac{c_a \rho L^4}{E K A G \tau^3} \frac{\partial^3 w}{\partial t^3} \\ &\quad - \frac{c_b \rho L^4}{E I K G \tau^3} \frac{\partial^3 w}{\partial t^3} - \frac{c_a c_b L^4}{E I K A G \tau^2} \frac{\partial^2 w}{\partial t^2} - \frac{\rho A L^4}{EI \tau^2} \frac{\partial^2 w}{\partial t^2} - \frac{c_a L^4}{EI \tau} \frac{\partial w}{\partial t} \\ &\quad + \frac{L}{EI} \frac{\partial^2}{\partial x^2} \int_0^t g(t-\tau) \left(-\frac{\rho L}{K G \tau^2} \frac{\partial^2 w}{\partial t^2} - \frac{c_a L}{K A G \tau} \frac{\partial w}{\partial t} + \frac{L}{EI} \frac{\partial^2 w}{\partial x^2} \right) \tau dt \end{aligned}$$

The Laplace transform is taken:

$$\begin{aligned} \left(1 - \frac{\tau G(s)}{EI s} \right) \frac{\partial^4 W}{\partial x^4} &= \left(\frac{\rho L^2}{E \tau^2} s^2 + \frac{\rho L^2}{K G \tau^2} s^2 + \frac{c_a L^2}{K A G \tau} s + \frac{c_b L^2}{EI \tau} s - \frac{\rho L^2}{K G E I \tau} G(s) s - \frac{c_a L^2}{K A G E I} G(s) + \frac{T L^2}{EI} \right) \frac{\partial^2 W}{\partial x^2} \\ &\quad + \left(-\frac{\rho^2 L^4}{E K G \tau^4} s^4 - \frac{c_a \rho L^4}{E K A G \tau^3} s^3 - \frac{c_b \rho L^4}{E I K G \tau^3} s^3 - \frac{c_a c_b L^4}{E I K A G \tau^2} s^2 - \frac{\rho A L^4}{EI \tau^2} s^2 - \frac{c_a L^4}{EI \tau} s \right) W \end{aligned}$$

And the final equation is:

$$\frac{\partial^4 W}{\partial x^4} = \frac{(P_1 s^2 + P_2 s^2 + A_d s + B_d s - P_2 C s - A_d C + T_s)}{\left(1 - \frac{C}{s} \right)} \frac{\partial^2 W}{\partial x^2} + \frac{(-P_1 P_2 s^4 - P_1 A_d s^3 - P_2 B_d s^3 - A_d B_d s^2 - s^2 - D_d s)}{\left(1 - \frac{C}{s} \right)} W$$

These models each incorporate a history kernel term, $G(s)$ (included as part of the dimensionless parameter C), with units of $\text{kg}\cdot\text{m}^3/\text{s}^3$. This term can take several forms, as shown in Table 1, and must be positive in order to model energy dissipation. In these simulations, the dissipation function used by Golla and Hughes [7] was used since their damping solution method incorporates a transfer function to model the system hysteresis. Although developed for finite element systems, this dissipation function is compatible with the distributed transfer function method. For this investigation, the Boltzmann time hysteresis formulation [6] was also used in the Euler-Bernoulli beam model as a comparison.

Table 1 Dissipation functions used for hysteretic damping term $G(s)$

Dissipation Function / History Kernel	Author, Year
$G(s) = \sum_{i=1}^n \frac{a_i s}{s + b_i}$	Biot, 1955 [7]
$G(s) = \frac{E_1 s^\alpha - E_0 b s^\beta}{1 + b s^\beta}, 0 < \alpha, \beta < 1$	Bagley and Torvik, 1981 [7]
$G(s) = a s \int_0^\infty \frac{\gamma(p)}{s+p} dp, \gamma(p) = \begin{cases} 1 \\ \beta - \alpha \end{cases}, \alpha < p < \beta$ 0 otherwise	Buhariwala, 1982 [7]
$G(s) = \frac{\alpha s^2 + \gamma s}{s^2 + \beta s + \delta}$	Golla and Hughes, based off of Biot's formula for $n=2$, 1985 [7]
$G(s) = \alpha \frac{s^2 + 2\sqrt{2}\delta s}{s^2 + 2\sqrt{2}\delta s + \delta}$	Inman, following the suggestion of Golla and Hughes and confirmed by Mctavish, 1989 [9]
$G(s) = \frac{\alpha}{\sqrt{-s}} \exp(\beta s)$	Banks and Inman, 1991, associated with Boltzmann damping [6]
$G(s) = \alpha \frac{1 - \exp(-s t_0)}{s t_0}$	Adhikari, 1998 [10]

DISTRIBUTED TRANSFER FUNCTION METHOD

The complexity of the Timoshenko equations of motion due to the added shear, rotary inertia and tension, and the inclusion of multiple damping terms make the final formulations computationally intense to solve. The distributed transfer function method (DTFM) is an exact method that poses the equation of motion as a transfer function matrix that can be manipulated to solve for the natural frequencies, displacements, and vibration response without having to assume a mode shape or approximate solution [8]. A desire to compare the effects due to the various damping terms (which may affect the cable response minutely) indicated that an exact method would be beneficial, since the small variations would not be lost in approximations.

To implement the distributed transfer function method, the equations of motion and boundary conditions are cast into a state-space form as follows:

$$\begin{aligned}\frac{\partial}{\partial x}\eta(x, s) &= F(s)\eta(x, s) + f(x, s) \\ M(s)\eta(0, s) + N(s)\eta(1, s) &= \gamma(s)\end{aligned}$$

where boundary conditions are incorporated through the M and N matrices, with pinned, clamped, or free end conditions all straightforward to implement, and

$$\eta = \begin{bmatrix} W(x, s) \\ \frac{\partial W(x, s)}{\partial x} \\ \frac{\partial^2 W(x, s)}{\partial x^2} \\ \frac{\partial^3 W(x, s)}{\partial x^3} \end{bmatrix}$$

$$M_{Pin} = \begin{bmatrix} 1 & 0 & 0 & 0 \\ 0 & 0 & EI + \frac{1}{s}G(s) & 0 \\ 0 & 0 & 0 & 0 \\ 0 & 0 & 0 & 0 \end{bmatrix}, N_{Pin} = \begin{bmatrix} 0 & 0 & 0 & 0 \\ 0 & 0 & 0 & 0 \\ 1 & 0 & 0 & 0 \\ 0 & 0 & EI + \frac{1}{s}G(s) & 0 \end{bmatrix}, M_{Clamp} = \begin{bmatrix} 1 & 0 & 0 & 0 \\ 0 & 1 & 0 & 0 \\ 0 & 0 & 0 & 0 \\ 0 & 0 & 0 & 0 \end{bmatrix}, N_{Clamp} = \begin{bmatrix} 0 & 0 & 0 & 0 \\ 0 & 0 & 0 & 0 \\ 1 & 0 & 0 & 0 \\ 0 & 1 & 0 & 0 \end{bmatrix},$$

Here, the M and N matrices describe the pinned or clamped ends of the cable section as noted in the subscript. In this case, there is no forcing function and initial conditions are uniformly zero, and the length of the beam section is normalized to 1. The $F(s)$ matrix is defined as follows, and the transfer function matrices for the viscously damped model and the two models with time hysteresis damping are shown below.

$$F(s) = \begin{bmatrix} 0 & 1 & 0 & 0 \\ 0 & 0 & 1 & 0 \\ 0 & 0 & 0 & 1 \\ d_0(s) & d_1(s) & \dots & d_k(s) \end{bmatrix}$$

with the last row of matrix entries are each defined as

$$d_k(s) = -\frac{a_k s^2 + b_k s + c_k}{a_n s^2 + b_n s + c_n}, k = 0, 1, \dots, n-1$$

where the a , b and c terms come from the form of the equations of motion:

$$\left\{ \left(\sum_{k=0}^n a_k \frac{\partial^k}{\partial x^k} \right) \frac{\partial^2}{\partial t^2} + \left(\sum_{k=0}^n b_k \frac{\partial^k}{\partial x^k} \right) \frac{\partial}{\partial t} + \left(\sum_{k=0}^n c_k \frac{\partial^k}{\partial x^k} \right) \right\} W(x, t) = f(x, t)$$

For the case of the Euler-Bernoulli beam equation and the fourth order Timoshenko beam equations derived in the previous section, the transfer function matrices are:

$$F_{EBTHyst} = \begin{bmatrix} 0 & 1 & 0 & 0 \\ 0 & 0 & 1 & 0 \\ 0 & 0 & 0 & 1 \\ \frac{(-s^2 - D_d s)}{1 - \frac{C}{s}} & 0 & \frac{T_s}{1 - \frac{C}{s}} & 0 \end{bmatrix}$$

$$F_{TimViscous} = \begin{bmatrix} 0 & 1 & 0 & 0 \\ 0 & 0 & 1 & 0 \\ 0 & 0 & 0 & 1 \\ (-P_1 P_2 s^4 - A_d P_1 s^3 - B_d P_2 s^3 - A_d B_d s^2 - s^2 - D_d s) & 0 & (P_1 s^2 + P_2 s^2 + A_d s + B_d s + T_s) & 0 \end{bmatrix}$$

$$F_{TimTHystW} = \begin{bmatrix} 0 & 1 & 0 & 0 \\ 0 & 0 & 1 & 0 \\ 0 & 0 & 0 & 1 \\ \frac{(-P_1 P_2 s^4 - A_d P_1 s^3 - B_d P_2 s^3 - A_d B_d s^2 - s^2 - D_d s)}{1 - \frac{C}{s}} & 0 & \frac{(P_1 s^2 + P_2 s^2 + A_d s + B_d s + T_s)}{1 - \frac{C}{s}} & 0 \end{bmatrix}$$

$$F_{TimTHystPsi} = \begin{bmatrix} 0 & 1 & 0 & 0 \\ 0 & 0 & 1 & 0 \\ 0 & 0 & 0 & 1 \\ \frac{(-P_1 P_2 s^4 - A_d P_1 s^3 - B_d P_2 s^3 - A_d B_d s^2 - s^2 - D_d s)}{1 - \frac{C}{s}} & 0 & \frac{(P_1 s^2 + P_2 s^2 + A_d s + B_d s - P_2 C s - A_d C + T_s)}{1 - \frac{C}{s}} & 0 \end{bmatrix}$$

The natural frequencies are determined by solving the eigenvalue problem; the eigenvalues of the system are the roots of the characteristic equation

$$\det[M(s) + N(s) * \exp(F(s) * L)] = 0$$

where the determinant is a symbolic expression containing s , which can be solved for through computer coding. The roots are of the form $s = j\omega_k$, $j = \sqrt{-1}$, $k = 1, 2, \dots$, where ω_k is the k th natural frequency of the system. Mode shapes for the system are determined by substituting the values for s back into the characteristic equation to solve for the displacement values (η) and then putting them into the solution equation

$$\eta(x, s) = \exp(F(s) * x) * \eta(0, s), \quad 0 \leq x \leq L$$

to get a function of x for each s value. It should be noted that the above procedures are for a single section of beam, and that modifications are required to solve the system for a set of subsystems linked together.

A key advantage of the distributed transfer function method (aside from needing fewer nodes than a similar finite element problem), is the ability to incorporate properties of the system that are dependent on the location. For example, research shows that the bending stiffness of a beam is variable when the beam is a multi-stranded cable [11]. Including an EI term that is dependent on the cable curvature is planned for future work.

RESULTS

For the results shown here, the modeled cable is assumed to be a uniform beam with properties similar to pure copper. Damping coefficients were chosen to give roughly similar changes in the natural frequencies, and will be the subject of a later study using experimental data. The cables were modeled with clamped ends on each side, and alpha and gamma dissipation function values were used from [12]. Table 2 gives the values for the nondimensional parameters for the various Euler Bernoulli cases and Table 3 lists the first four natural frequencies for each case. Table 4 and 5 provide the program inputs and frequency results for the first four modes for the various Timoshenko beam cases. Figure 3 is a frequency response comparison for the Euler-Bernoulli beam model showing the undamped model, a lightly viscously damped model, and a time hysteresis damped model incorporating the dissipation function used by Golla and Hughes. Figure 4 compares the hysteretic damping from the Boltzmann function with the undamped and viscously damped Euler Bernoulli cases.

Table 2 Nondimensional values used for Euler-Bernoulli model simulations, based on properties of single copper wire and Boltzmann and Golla-Hughes dissipation functions

Euler Bernoulli Values		Undamped	Viscously Damped	Time Hysteresis, Boltzmann Function	Time Hyst., Golla-Hughes Function
Dimensionless Time Parameter	τ	0.2294	0.2294	0.2294	0.2294
Tension	T_s	0	0	0	0
Hysteretic Damping Coefficient	$C * G(s)$	0	0	$0.0736 * G(s)$	$0.0736 * G(s)$
Dissipation Function	$G(s)$	0	0	$\frac{1.36}{\sqrt{-s}} * \exp(\beta * s)$	$\frac{1.36s^2 + 1.5e4s}{s^2 + 1s + 1.5e6}$
Viscous Damping Term	D	0	1.6794 ($c_d=1.2$)	0	0

Table 3 First four natural frequencies for undamped and damped Euler Bernoulli models

Mode #	Euler Bernoulli Undamped	EB Viscously Damped	EB Time Hyst, Golla-Hughes Function	EB Time Hyst, Boltzmann Function, $\beta = 1$	EB Time Hyst, Boltzmann Function, $\beta = 5$
1	22.3733	22.3599	21.5067	22.3831	22.3776
2	61.6728	61.6863	58.6529	61.6751	61.6668
3	120.9034	120.9194	103.86, 115.7077, 122.21*	120.9000	120.8995
4	199.8594	199.8747	203.9654	199.8609	199.8564

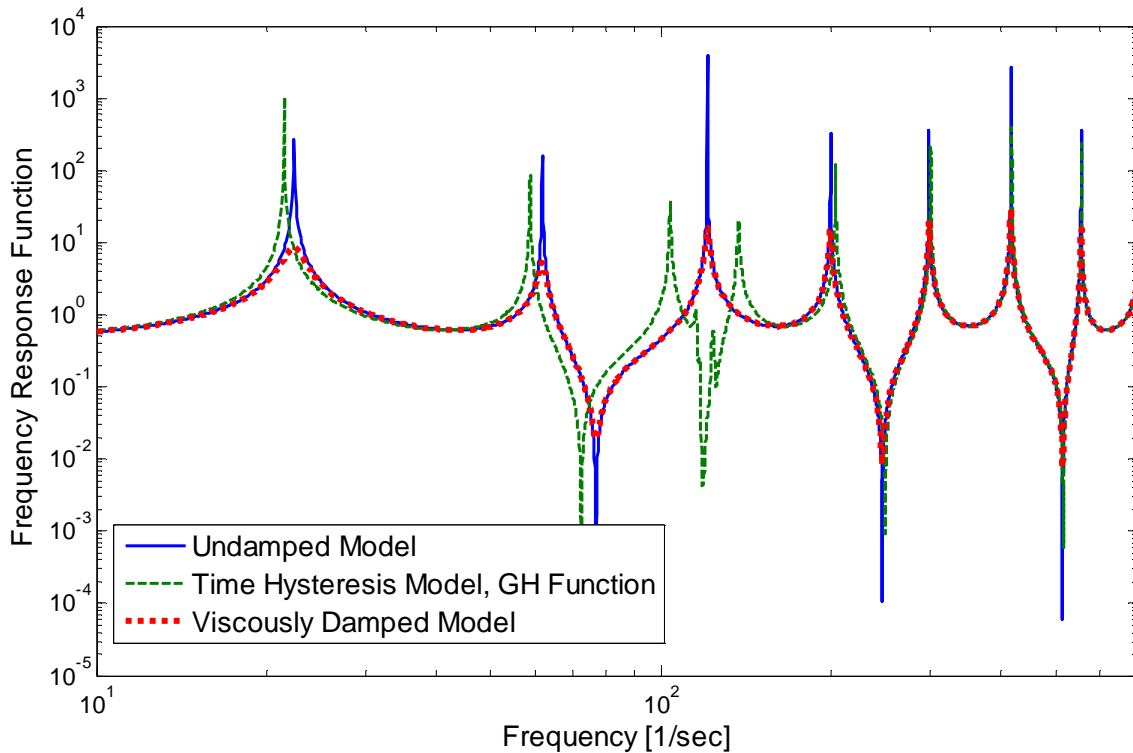


Fig. 3 Euler Bernoulli beam model compared to viscously damped and Golla Hughes time hysteresis damped models

* When calculating the natural frequencies, use of the Golla-Hughes function resulted in additional frequencies around the third mode, also shown in Figure 3. Although the intent of this work was to find damping mechanisms that would result in

additional modes, it is likely that these modes are due to numerical instability in the solution step. Although the DTF method is intended to be exact, a numeric solver was used to find the natural frequencies based on setting the determinant of the system transfer function equal to zero. With higher damping values, this effect was more pronounced, and will require further study to determine the stability limits of the damping functions.

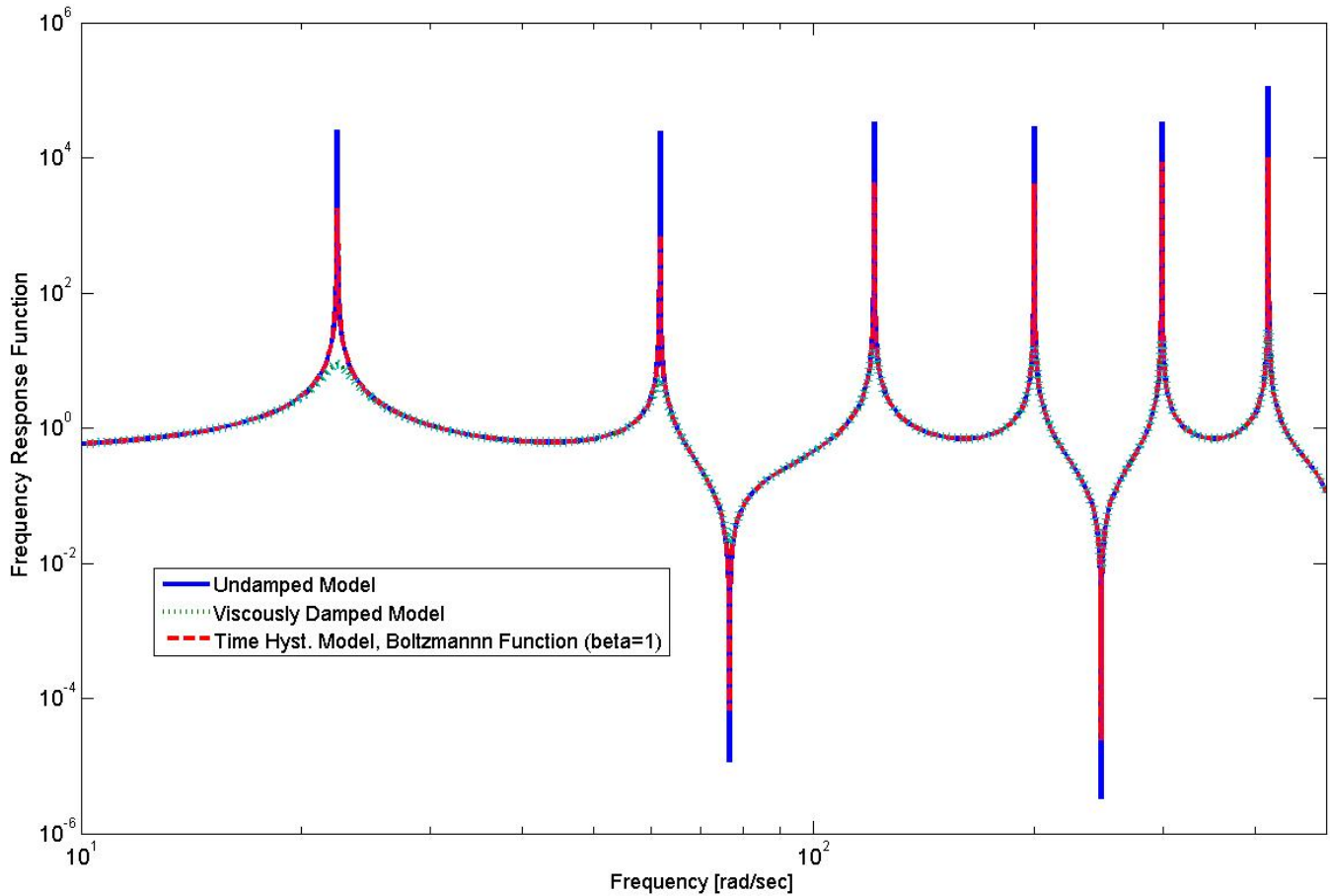


Fig. 4 Comparison of undamped Euler Bernoulli model with Boltzmann time hysteresis damping and viscous damping

In the case of the Boltzmann time hysteresis damping, the damping effects were nearly identical to viscous damping. The time hysteresis models did provide different damping magnitudes and, in some cases, shifted frequencies, but additional modes that could arise from hysteretic damping were not evident. The results from this work indicate that additional damping coordinates (as proposed in the Golla-Hughes-McTavish method) will be necessary to predict damping behavior; including just the dissipation functions is not sufficient for response prediction. More positively, adding time hysteresis dissipation functions to the Euler Bernoulli beam model did not extend computational time excessively.

Although a decrease in natural frequencies was expected for viscously damped beams, investigation into the distributed transfer function method showed that the viscous damping is not necessarily modal damping, and similar problems in the literature show a decrease in the first natural frequency only [8]. However, the amplitude of the response is reduced for all frequency values, showing significant damping. As Figure 1 showed, the slack cable which experiences greater damping had frequencies that shifted both higher and lower than its tensioned counterparts. Results for the Euler Bernoulli and Timoshenko beams showed that time hysteresis damping did not have a constant higher or lower shift of the natural frequencies, and may be best to model the frequency shifts due to the damping inherent in a slack cable. Some stability issues arose (for example, the disparity between the fourth mode value for the Timoshenko time hysteresis case) for certain

combinations of damping coefficients, and more research is needed to determine the appropriate range of coefficients to characterize the physical damping mechanisms of cables.

Table 4 Nondimensional values used for Timoshenko model investigation, based on properties of single copper wire and Golla-Hughes dissipation functions

Timoshenko Values	Undamped	Viscously Damped, $c_a = 5$	Viscously Damped, $c_a = c_b = 0.5$	Time Hyst. on W	Time Hyst. on Psi
A_d	0	2.9425E-05	2.9425E-06	0	0
B_d	0	0	0.6997	0	0
P_1	1.4556E-06	1.4556E-06	1.4556E-06	1.4556E-06	1.4556E-06
P_2	4.2052E-05	4.2052E-05	4.2052E-05	4.2052E-05	4.2052E-05
C	0	0	0	0.0736* $G(s)$	0.0736* $G(s)$
Golla-Hughes Function	0	0	0	$\frac{1.36s^2 + 1.5e4s}{s^2 + s + 1.5e4}$	$\frac{1.36s^2 + 1.5e4s}{s^2 + s + 1.5e4}$
D_d	0	6.9974	0.6997	0	0
T_s	0	0	0	0	0
τ	0.2294	0.2294	0.2294	0.2294	0.2294

Table 5 First four natural frequencies for undamped and damped Timoshenko beam models

Mode #	Timoshenko Undamped	Timoshenko Viscously Damped $c_a = 5, c_b = 0$	Timoshenko Viscously Damped $c_a = 0.5, c_b = 0.5$	Timoshenko Time Hyst. on W, Golla-Hughes Function	Timoshenko Time Hyst. on Psi, Golla-Hughes Function
1	22.3726	22.1498	19.4533	21.5059	21.5060
2	61.6649	61.9026	47.2953	58.6455	58.6460
3	120.8696	121.1532	147.6919	115.7036	115.7260
4	199.7625	200.0325	221.0475	203.8723	137.2000

In the Timoshenko beam cases, the rotational damping coefficient c_b has a much greater effect on the natural frequency change than the bending damping coefficient c_a . This is likely due to the relative weight of the terms; when the rotational damping coefficient is non-dimensionalized, it is 5 orders of magnitude larger than the bending coefficient, which indicates that the inclusion of the rotational damping term is necessary and supports the decision to model cables with Timoshenko beams despite the increased complexity.

The use of Timoshenko beam models rather than Euler Bernoulli models provided the largest increase in computation time, taking significantly longer to compute whether time hysteresis damping was included or not. However, existing literature [5] emphasizes the need to include shear effects, and the importance of the rotational damping factor in these results indicates that the Timoshenko model is necessary, despite the additional time required. Time hysteresis damping added some complexity, but was minimal as compared to the complexity of the Timoshenko formulation.

While the authors had hoped that the use of dissipation functions in conjunction with the DTFM method could capture the nuances of cable damping, including time hysteresis without adding additional dissipation coordinates does not seem to improve significantly upon viscous damping as a damping predictor. The next step is to combine the Golla-Hughes-McTavish method of additional dissipation coordinates with the DTFM method and Timoshenko beam formulation if possible.

Since preliminary cable experiments were performed, many factors arose that indicated the need for more focused and detailed experiments. The data shown in Figure 1 is from small diameter cables that bear little resemblance to the space

flight cables that we are interested in modeling, and do not show much variation in construction or jacket type. In the simulations run above, the various damping coefficients and dissipation function constants were chosen arbitrarily based on published data and trial and error. To predict the cable response, these values must be correlated to cable properties such as modulus of elasticity and rigidity, cable geometry, cable construction, and jacketing, which forms the basis for our ongoing investigation.

CONCLUSION AND FUTURE WORK

Various damping and stiffness models were examined to see if they could predict the behavior of cables. Viscous damping and time hysteresis damping formulations were added to beam models, and the damped natural frequencies were calculated using the distributed transfer function method. Adding hysteretic dissipation functions alone did not vary the response significantly from viscous damping models, and incorporating additional dissipation coordinates must be investigated. Adding hysteresis functions to the equations of motion did not significantly increase computation time, although the additional complexity of the shear and rotational inertia terms for the Timoshenko model did. The use of the Timoshenko beam model rather than the Euler Bernoulli beam model was supported based on the magnitude of the non-dimensionalized rotational damping coefficient and previous studies [5].

The logical next step is to incorporate the Golla-Hughes-McTavish method of additional damping coordinates to improve the models. Then, we will perform experiments with spaceflight cables to correlate the damping coefficients to cable properties and validate the proposed damping models. We have determined that the additional time required for the more complex damping and Timoshenko terms is not excessive, and may lead to results that can more accurately model the erratic behavior of slack space flight cables. Future directions include comparing spatial hysteresis damping, and incorporating variable bending stiffness as investigated in [11], where the bending stiffness is related to the curvature of the cable at any given point in time and space.

ACKNOWLEDGEMENTS

This work was supported by a NASA Office of the Chief Technologist's Space Technology Research Fellowship. The first author thanks NASA for generous support and the Virginia Space Grant Consortium for additional funding. The third author gratefully acknowledges the support of AFOSR Grant number FA9550-10-1-0427 monitored by Dr. David Stargel. Part of this research was carried out at the Jet Propulsion Laboratory, California Institute of Technology, under a contract with the National Aeronautics and Space Administration.

REFERENCES

- [1] Costello, G.A. *Theory of Wire Rope*, 2nd Ed. New York: Springer, 1997.
- [2] Jolicoeur C., and Cardou A., "Semicontinuous Mathematical Model for Bending of Multilayered Wire Strands," *Journal of Engineering Mechanics*, Vol. 122(7), pp. 643–650, 1996.
- [3] Spak, K., and Inman, D., "Model Development for Cable-Harnessed Beams," 2012 Virginia Space Grant Consortium Student Research Conference, Williamsburg, VA, April 2012.
- [4] Banks, H.T., Fabiano, R.H., Wang, Y., Inman, D.J., and Cudney, H., "Spatial Versus Time Hysteresis in Damping Mechanisms," *Proceedings of the 27th Conference on Decision and Control*, Austin, Texas, pp. 1674-1677, Dec. 1988.
- [5] Goodding, J.C., Griffiee, J.C., and Ardelean, E.V. "Parameter Estimation and Structural Dynamic Modeling of Electrical Cable Harnesses on Precision Structures," 49th AIAA/ASME/ASCE/AHS/ASC Structures, Structural Dynamics, and Materials Conference, April 2008.
- [6] Banks, H.T., and Inman, D. J., "On Damping Mechanisms in Beams," *Journal of Applied Mechanics*, Vol. 58., Sept., pp. 716-723, 1991.

- [7] Golla, D.F., and Hughes, P.C., "Dynamics of Viscoelastic Structures- A Time-Domain, Finite Element Formulation," *Journal of Applied Mechanics*, Vol. 52, Dec., pp. 897-906, 1985.
- [8] Yang, B., and Tan, C.A., "Transfer Functions of One-Dimensional Distributed Parameter Systems," *Journal of Applied Mechanics*, Vol. 59, Dec., pp. 1009-1014, 1992.
- [9] Inman, D.J., "Vibration Analysis of Viscoelastic Beams by Separation of Variables and Modal Analysis," *Mechanics Research Communications*, Vol. 16(4), pp. 213-218, 1989.
- [10] Adhikari, S. "Damping Models for Structural Vibration," Thesis. Cambridge University, 2000.
- [11] Papailiou, K.O., "On the Bending Stiffness of Transmission Line Conductors," *IEEE Transactions on Power Delivery*, Vol. 12(4), pp. 1576- 1588, 1997.
- [12] Sciulli, D. "Dynamics and Control for Vibration Isolation Design," Thesis. Virginia Tech, 1997.